Supporting Information

Gonzalez et al. 10.1073/pnas.1308953111

Materials and Methods

Cell Culture. The breast cancer cell line MDA-MB-231 and the immortalized human mammary epithelial cell line MCF10A were obtained from the American Type Culture Collection and grown under recommended conditions. The SUM149 breast cancer cell line was obtained from the S. Ethier laboratory (Karmanos Cancer Institute, Detroit) and cultured as previously reported (1). Human mammary epithelial cells were purchased from ScienCell Research Laboratories (catalog no. 7610) and maintained following the manufacturer's instructions. These cells were delivered frozen after being isolated from normal human breast tissue and being cryopreserved at first passage.

Two fresh breast tumor tissue samples were obtained through the Tissue Procurement Service at the University of Michigan (Institutional Review Board No. HUM00050330). The samples were immediately processed in the laboratory. A portion was formalin-fixed and paraffin-embedded for staining with hematoxylin/eosin (H&E) and immunohistochemical staining with anti-Enhancer of Zeste Homolog 2 (EZH2) (Cell Signaling; catalog no. 5246; 1:150); see *Human Breast Cancer Samples and Immunohistochemical Staining* for a detailed staining protocol. Another portion was processed to a single-cell suspension by manually mincing the tumor followed by dissociation in a collagenase-hyaluronidase solution (StemCell Technologies; catalog no. 07912). Next, red blood cells were lysed with RBC Lysis Solution (Qiagen; catalog no. 158902). For further purification, the tissue was treated with Trypsin-EDTA (GIBCO; catalog no. 25200-056) and then DNase1 (StemCell Technologies; catalog no. 07900) and finally filtered through a 40-μm cell strainer. Cells were cultured in Mammary Epithelial Cell Medium (ScienCell; catalog no. 7611) completed with Mammary Epithelial Cell Growth Supplement and penicillin–streptomycin (ScienCell; catalog nos. 7652 and 0503).

Vectors, Viral Infections, and Inhibitors. EZH2 knockdown (KD) using stable short-hairpin interfering RNA in lentivirus was completed as previously reported (2). For targeting *EZH2* (NM_152998 NCBI), the shRNA oligo ID V2LHS_17507 was used and corresponded to RHS4430-99139126 from Open Biosystems. This oligo was cloned into a pLKO.1-Puro vector and packaged into lentiviral particles at the University of Michigan Vector Core. A lentivirus containing a plasmid encoding a scrambled shRNA oligo was used for control. Cells were transduced and selected for antibiotic resistance with puromycin (Sigma-Aldrich; catalog no. P9620). Conditional overexpression of EZH2 in MCF10A cells (pLVX-EZH2) was achieved through a doxycycline-inducible system previously developed in our laboratory (3). Transient EZH2 overexpression was also achieved through infection with a myc-tagged plasmid cytomegalovirus promoter encoding either wild-type or specific-deletion mutants of EZH2 for 48 h, as previously reported (4, 5).

For the transient ectopic expression of the EZH2 point mutant (EZH2-H689A), we used an expression plasmid containing full-length cDNA under the control of a CMV promoter, kindly provided by K. Yeung (University of Toledo, Toledo, OH) (6–8).

NOTCH1 was down-regulated using NOTCH1 (NM_017617) siRNA (Sigma-Aldrich; catalog no. EHU150431-50UG), in cell culture using oligofectamine (Invitrogen; catalog no. 12252-011), following the manufacturer's instructions. NOTCH1 signaling inhibition was completed by treating MCF10A cells with γ-secretase inhibitor (GSI) (Calbiochem; catalog no. 565750) for 3 d at 17 nM in cell culture and for 7 d at 1.7 nM in mammosphere assays.

To reconstitute NOTCH1 intracellular domain (NICD1) expression, primary tumor-derived cells expressing either scrambled control or EZH2-targeted shRNA were transiently transduced with constitutively active NICD1 in a retrovirus vector (9). Cells were plated for mammosphere assays 72 h post-virus transduction.

A pGreenFire1-NOTCH plasmid that expresses a destabilized copGFP reporter and firefly luciferase under the control of four NOTCH transcriptional response elements and a minimal CMV promoter (System Bioscience; catalog no. TR020PA-1) was transiently expressed in a lentiviral vector for the NOTCH transcriptional activity reporter assays.

Immunoblots. Western blot analyses were carried out with 100 μg of whole-cell extract derived as previously reported (3). Membranes were blocked and incubated with primary antibodies in 4% (vol/vol) milk (Sigma-Aldrich; catalog no. A3059) in Tris-buffered saline with Tween-20 (Bio-Rad; catalog no. 161-0372; with 0.05% Tween-20) at 4 °C overnight. Mouse monoclonal antibodies β-Actin–HRP (Santa Cruz; catalog no. 47778), anti-GAPDH (Abcam; catalog no. ab9484), and anti–α-Tubulin (Sigma-Aldrich; catalog no. T9026) were used to confirm equal loading. Primary antibodies from Cell Signaling included rabbit monoclonal antibodies anti-EZH2 (catalog no. 5246), anti-Cyclin D1 (catalog no. 2978), anti-HES1 (catalog no. 11988), anti-Suz12 (catalog no. 3737), rabbit polyclonal anti-Histone H3 (catalog no. 9715), and mouse monoclonal anti–Myc-Tag (catalog no. 2276). The mouse monoclonal antibodies anti-NOTCH1 (Santa Cruz Biotechnology; catalog no. SC-32745), anti-Histone H3, trimethyl K27 (Abcam; catalog no. ab6002), and anti-EED (Abcam; catalog no. ab4469) were used.

Mammosphere Assays. Single-cell dissociation for mammosphere formation assays was performed following established protocols with SUM149, MDA-MB-231, MCF10A, and patient-derived tumor cells plated at a density of 1×10^4 cells/mL (10). Mammospheres were cultured in MammoCult Human Basal Medium with added Proliferation Supplement (StemCell Technologies; catalog nos. 05621 and 05622) on Costar Ultra Low Attachment tissue culture plates (Corning; catalog no. 3471). At the end of 7 d, for both primary and secondary generations and mammosphere sizes and numbers were determined using a Leica inverted microscope. Size was measured as the widest diameter with the scale bar. All experiments were performed in triplicate.

Signaling Microarrays. Notch signaling Targets PCR Array (catalog no. PAHS-2597) and Stem Cell Signaling PCR Array (catalog no. PAHS-0477) from SA Biosciences were used to identify the gene expression profiles of aldehyde dehydrogenase 1 ($ALDH1^+$) SUM149 control and EZH2 KD cells. The arrays were performed in triplicate per each condition.

Quantitative RT-PCR, Chromatin Immunoprecipitation, and Rechromatin Immunoprecipitation Assays. Quantitative real-time reverse transcription–PCR (RT-PCR) amplifications were carried out with 1 μg of total RNA isolated from the indicated breast cells and conditions. Reactions were performed in triplicate using an Applied Biosystems StepOnePlus RT-PCR System available in the Michigan MicroArray Core with Qiagen primers and SYBR Green Master Mix (Applied Biosystems; catalog no. 4309155). All primers were purchased from Applied Biosystems: GAPDH (catalog no. Hs99999905_m1), EZH2 (catalog no. Hs00544830_m1), and

NOTCH1 (catalog no. Hs01062011_m1). All mRNA levels are expressed as relative to GAPDH mRNA levels.

The ChIP-IT Express Enzymatic kit and Re-ChIP-IT (Active Motif; catalog nos. 53009 and 53016, respectively) were used following the manufacturer's instructions. Antibodies were used at the manufacturer's recommended dilutions and included anti-EZH2, anti-Histone H3K27me2 me3, anti-SUZ12, anti-H3K4me2, anti-RelA (Active Motif; catalog nos. 39875, 39535, 39877, 39679, and 39369), anti-SET1 (Abcam; catalog no. ab70378), anti-RNA Polymerase II (Fisher; catalog no. 05-623), and anti-RelB (Santa Cruz; catalog no. sc-226). The following chromatin immunoprecipitation (ChIP)-Re-ChIP qPCR promoter primers were purchased from SABiosciences: for NOTCH1: GPH1027067(−)01A, GPH1027067(−)02A, GPH1027067(−)03A, GPH1027067(−)04A, GPH1027067(−)05A; and for GAPDH: GPH110001C(+)01A. The *MYT1* promoter primers used as a positive control for EZH2 binding were made as previously reported (11). ChIP and Re-ChIP assays are representative of three independent experiments.

Flow Cytometry. ALDEFLUOR assay was used for detection of the stem cell population using the ALDEFLUOR kit (StemCell Technologies; catalog no. 01700) following the manufacturer's instructions. Stem cell populations were also measured by labeling 1×10^6 cells with either anti-CD44 conjugated to allophycocyanin (APC) and anti-CD24 conjugated to R-phycoerythrin (PE) (BD Biosciences; catalog nos. 559942 and 555428) or anti-CD49f conjugated to APC (eBioscience; catalog no. 17-0495) and anti-ESA conjugated to PE (Biolegend; catalog no. 118215) at the manufacturer's recommended dilutions. For NOTCH reporter assays, 1×10^6 cells transduced with the NOTCH reporter lentivirus (described above) were subjected to flow cytometry to determine the percentage of GFP positive cells. All flow cytometric analyses were completed using the University of Michigan Flow Cytometry Core in triplicate.

Animal Studies. All procedures were conducted in accordance with the National Institutes of Health *Guide for the Care and Use of Laboratory Animals* (12) and were approved by the University Committee on Use and Care of Animals (UCUCA) at the University of Michigan (Prococol No. 00005009). For tumorigenicity experiments, 10-wk-old severe combined immunodeficient mice (The Jackson Laboratory) were used. SUM149 cells expressing EZH2-targeted or scrambled shRNA, sorted into $ALDH1^+$ and $ALDH1^-$ groups, were orthotopically injected into the mammary fat pad at a concentration of 1×10^4 cells in 40 mice ($n = 10$ per group). Tumor size was measured twice weekly until tumors reached 2 cm^3 [tumor volume = (length × $width^2$)/2], at which time, mice were killed.

To generate $EZH2^+$;neu and $EZH2^{wt}$;neu transgenic mice, female mouse mammary tumor virus (MMTV)-neu mice [The Jackson Laboratory; FVB/N-Tg(MMTVneu)202Mul/J] were bred with male heterozygous EZH2 transgenic mice previously developed in our laboratory using synchronized breeding methods (13). Mammary glands were excised at 8 wk, at 16 wk, and when tumors reached 2 cm^3. Mammary gland whole mounts were prepared by mounting the abdominal mammary fat pads on glass slides and processed following established protocols (13, 14). In brief, glands were excised, dehydrated, stained with alum carmine, stored in methyl salicylate, and mounted with Permount. Mammary gland tissue samples for histological analysis were fixed overnight in 10% neutral buffered formalin (Sigma-Aldrich; catalog no. HT501128), processed through graded alcohols, cleared in xylene, and embedded in paraffin. Tissues were sectioned at 5 μm and placed on charged slides. Slides were H&E-stained and subjected to immunohistochemistry as described below.

Mammary transplantation experiments were performed to assess the effect of EZH2 overexpression on in vivo mammary-repopulating capacity and stem cells (15). Mammary glands of $EZH2^+$;neu and $EZH2^{wt}$;neu female 8-wk-old transgenic mice underwent tissue dissociation and subjected to fluorescence-activated cell sorting (FACS) analyses of the lineage negative (Lin^-) populations using CD49f and ESA markers. These markers used in combination have been shown to identify stem and progenitor cells in human and in MMTV-neu mammary glands (16, 17). Stem cells (Lin^- ESA^{med} $CD49f^{high}$) and progenitors (Lin^- ESA^{high} $CD49f^{med}$) from 15 mice were independently injected (5,000 cells per group) in the mammary fat pad of female 3-wk-old FBV mice following the protocol for xenotransplantation described by Guo et al. (15). After 5 wk of observation, outgrowths from both groups were analyzed by FACS and histology. All mouse tissues were formalin-fixed and paraffin-embedded for H&E staining and immunohistochemical staining with anti-EZH2 (Cell Signaling; catalog no. 5246; 1:2,000), anti-Ki67 (Fisher; catalog no. RM-9106, 1:2,000), phospho-STAT3 (Cell Signaling; catalog no. 9145; 1:100), anti-NOTCH1/N-Terminus (Fisher; catalog no. 07-1232; 1:600), or anti-NOTCH1 (Epitomics; catalog no. 1935-1; 1:300). Image analysis and quantification of EZH2, NICD1, phospho-STAT3, and Ki-67 expression was completed using Framework for Image Dataset Analysis, a custom open source image analysis software package for the analysis of RGB color image datasets. Additional information can be found at http://bui3.win.ad.jhu.edu/frida.

To immunostain mouse mammary glands using dual immunohistochemistry for CD49f/ESA and CD49f/CD61, slides were deparaffinized in xylene and rehydrated through graded alcohols. Heat-induced epitope retrieval (HIER) was performed in the Decloaking Chamber (Biocare Medical) with Target Retrieval (pH 6.0; DakoCytomation). Slides were incubated in 3% hydrogen peroxide for 5 min to quench endogenous peroxidases. Anti-CD49f (Novus Biologicals; catalog no. NBP1-85747; 1:800) was applied and incubated for 1.5 h at room temperature. Anti-rabbit $Envision^+$ HRP Labeled Polymer (DakoCytomation) applied for 30 min at room temperature was used to detect the antibody. HRP staining was visualized with the DAB^+ Kit (DakoCytomation). Slides were denatured after diaminobenzidine (DAB) development and incubated in Rodent Block M (Biocare Medical) for 30 min at room temperature. Either anti-ESA (Novus Biologicals; catalog no. NB110-56958; 1:2,700) or anti-CD61 (Epitomics; catalog no. 2264-1; 1:600) was applied to the slides and incubated for 1.5 h at room temperature. Rabbit on Rodent AP-Polymer (Biocare Medical) applied for 15 min at room temperature was used to detect the antibody. AP staining was visualized with Warp Red (Biocare Medical). Negative control slides were run. Slides were counterstained in hematoxylin, blued in running tap water, and mounted with Clear Mount. CD49f was visualized as brown and CD61 and ESA as red.

Human Breast Cancer Samples and Immunohistochemical Staining. Three high-density tissue microarrays (TMAs) containing triplicate samples of 143 human primary invasive breast carcinomas developed and previously characterized by our group were used (4). The TMAs were subjected to immunohistochemistry to detect EZH2, NICD1, CD44, and CD24 proteins. Five-micron-thick paraffin-embedded sections were deparaffinized in xylene and rehydrated through graded alcohols to water. HIER was performed in the Decloaking Chamber (Biocare Medical) with Target Retrieval (pH 6.0; DakoCytomation). Slides were incubated in 3% hydrogen peroxide for 5 min to quench endogenous peroxidases. Anti-EZH2 (BD Biosciences catalog no. 612667 or Cell Signaling catalog no. 5246; 1:150–300), anti-NOTCH1/N-Terminus (Fisher; catalog no. 07-1232; 1:600), or an antibody mixture containing anti-CD44 (Abcam; catalog no. ab51037; 1:400) and anti-CD24 (Biocare Medical; catalog no. CM323; 1:100) were incubated with the TMAs for 1.5 h at room temperature. Antibodies were detected with either anti-rabbit or

anti-mouse Envision$^+$ HRP Labeled Polymer (DakoCytomation) for 30 min at room temperature or MACH 2 Double Stain 2 (Biocare Medical) for 20 min at room temperature. HRP staining was visualized with the DAB$^+$ Kit (DakoCytomation). AP staining was visualized with the Warp Red Kit (Biocare Medical). Negative control slides were run. Slides were counterstained in hematoxylin, blued in running tap water, dehydrated through graded alcohols, cleared in xylene, and then mounted with Permount. Nuclear expression of EZH2 was considered high or low based on staining intensity and percentage of tumor cells staining, based on a previously validated scoring system (4). NICD1 staining was interpreted as positive when it was expressed in the nuclei of cancer cells or negative when no nuclear staining was observed. Dual immunostaining for CD44 and CD24 proteins was evaluated as positive or negative based on detection of each protein in the cancer cells. CD44 was visualized as red and CD24 as brown.

Statistics. *P* values were obtained using Student's *t* test unless specified otherwise.

1. Kleer CG, Zhang Y, Pan Q, Merajver SD (2004) WISP3 (CCN6) is a secreted tumor-suppressor protein that modulates IGF signaling in inflammatory breast cancer. *Neoplasia* 6(2):179–185.
2. Gonzalez ME, et al. (2009) Downregulation of EZH2 decreases growth of estrogen receptor-negative invasive breast carcinoma and requires BRCA1. *Oncogene* 28(6): 843–853.
3. Gonzalez ME, et al. (2011) Histone methyltransferase EZH2 induces Akt-dependent genomic instability and BRCA1 inhibition in breast cancer. *Cancer Res* 71(6): 2360–2370.
4. Kleer CG, et al. (2003) EZH2 is a marker of aggressive breast cancer and promotes neoplastic transformation of breast epithelial cells. *Proc Natl Acad Sci USA* 100(20): 11606–11611.
5. Cao Q, et al. (2008) Repression of E-cadherin by the polycomb group protein EZH2 in cancer. *Oncogene* 27(58):7274–7284.
6. Kuzmichev A, Nishioka K, Erdjument-Bromage H, Tempst P, Reinberg D (2002) Histone methyltransferase activity associated with a human multiprotein complex containing the Enhancer of Zeste protein. *Genes Dev* 16(22):2893–2905.
7. Kim E, et al. (2013) Phosphorylation of EZH2 activates STAT3 signaling via STAT3 methylation and promotes tumorigenicity of glioblastoma stem-like cells. *Cancer Cell* 23(6):839–852.
8. Ren G, et al. (2012) Polycomb protein EZH2 regulates tumor invasion via the transcriptional repression of the metastasis suppressor RKIP in breast and prostate cancer. *Cancer Res* 72(12):3091–3104.
9. Pui JC, et al. (1999) Notch1 expression in early lymphopoiesis influences B versus T lineage determination. *Immunity* 11(3):299–308.
10. Dontu G, et al. (2003) In vitro propagation and transcriptional profiling of human mammary stem/progenitor cells. *Genes Dev* 17(10):1253–1270.
11. Anonymous (2013) Methylation by EZH2 activates STAT3 in glioblastoma. *Cancer Discov* 3(7):OF21.
12. National Research Council (US) Committee on Care and Use of Laboratory Animals (2011) *Guide for the Care and Use of Laboratory Animals* (National Academies Press, Washington, DC), 8th Ed.
13. Li X, et al. (2009) Targeted overexpression of EZH2 in the mammary gland disrupts ductal morphogenesis and causes epithelial hyperplasia. *Am J Pathol* 175(3): 1246–1254.
14. Jones FE, Jerry DJ, Guarino BC, Andrews GC, Stern DF (1996) Heregulin induces in vivo proliferation and differentiation of mammary epithelium into secretory lobuloalveoli. *Cell Growth Differ* 7(8):1031–1038.
15. Guo W, et al. (2012) Slug and Sox9 cooperatively determine the mammary stem cell state. *Cell* 148(5):1015–1028.
16. Lim E, et al.; kConFab (2009) Aberrant luminal progenitors as the candidate target population for basal tumor development in BRCA1 mutation carriers. *Nat Med* 15(8): 907–913.
17. Lo PK, et al. (2012) CD49f and CD61 identify Her2/neu-induced mammary tumor-initiating cells that are potentially derived from luminal progenitors and maintained by the integrin-TGFβ signaling. *Oncogene* 31(21):2614–2626.

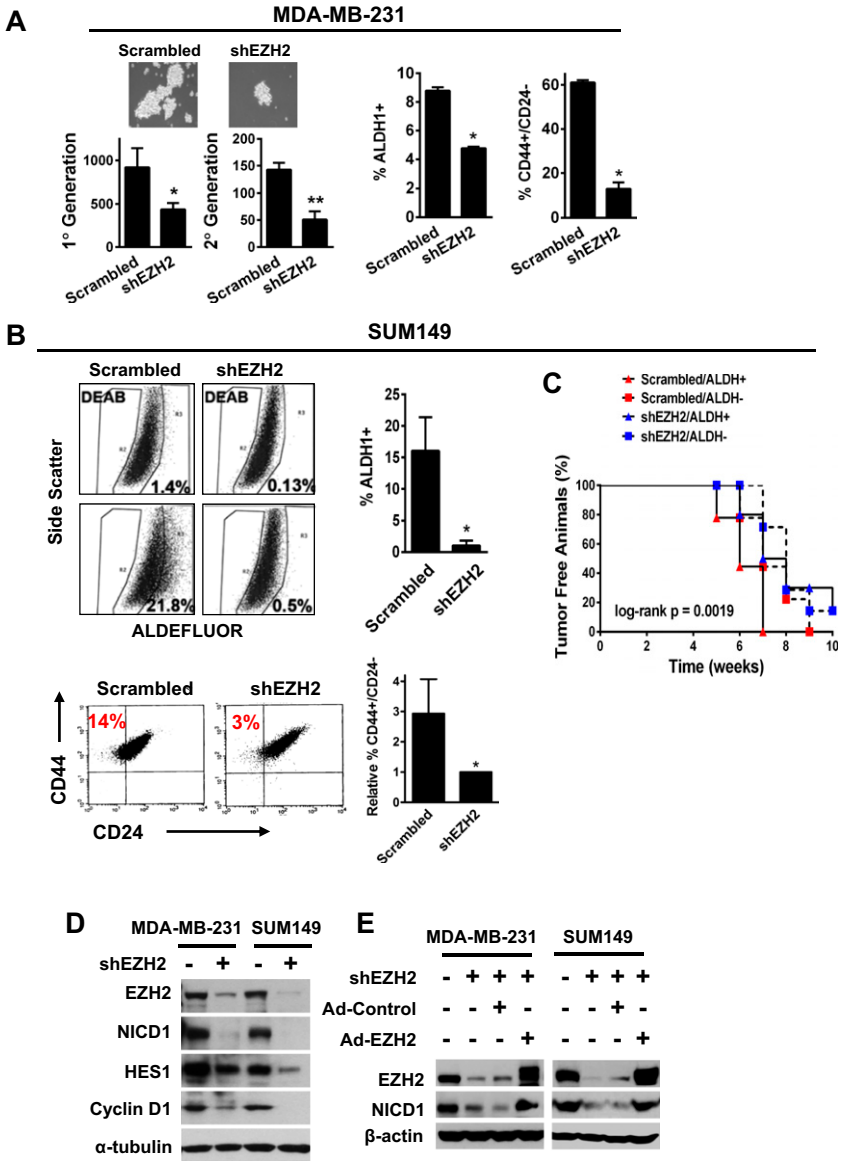

Fig. S1. (Continued)

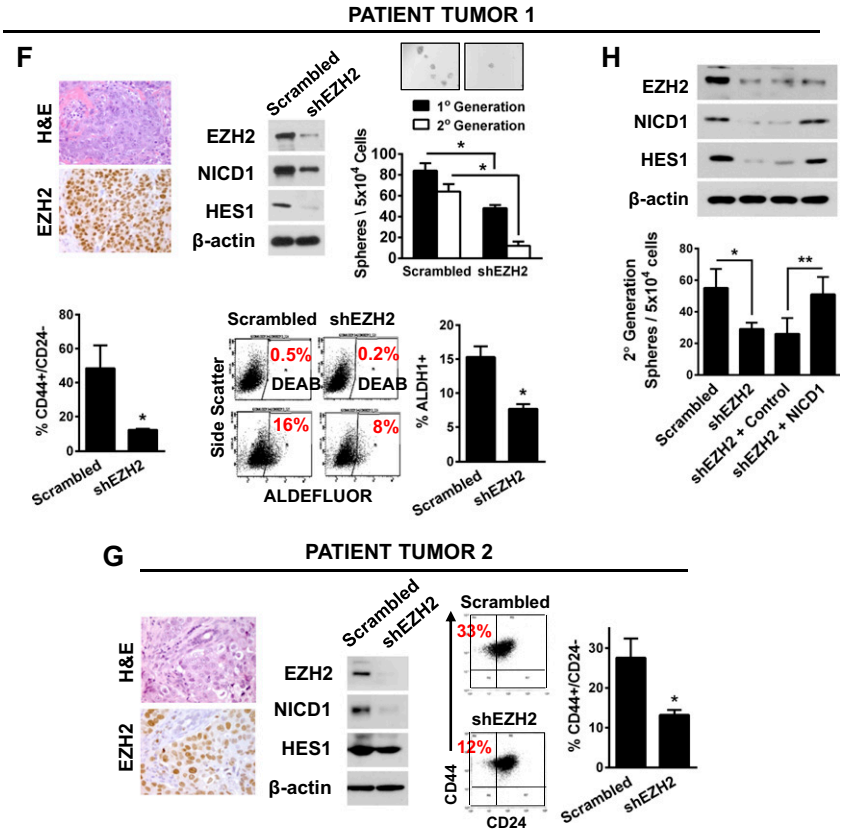

Fig. S1. Effect of EZH2 KD on breast cancer tumor-initiating cell (TIC) population. (*A*, *Left*) EZH2 KD in MDA^{-} MB-231 cells reduces the number of spheres compared with controls. Representative images of the spheres. (Magnification: 200×.) Average number of primary and secondary generation spheres ± SD per 5×10^4 plated cells (*t* test: $*P = 0.03$; $**P = 0.0003$). (*A*, *Right*) EZH2 KD in MDA-MB-231 cells decreases the percentage of ALDH1^{+} cells and the CD44^{+}/CD24^{-} population compared with controls ± SD (*t* test, $*P < 0.0001$). (*B*) EZH2 KD in SUM149 cells decreases the ALDH1^{+} population and the relative CD44^{+}/CD24^{-} population compared with controls (*t* test, $*P < 0.001$). (*C*) EZH2 KD decreases the tumor onset of SUM149 ALDH1^{+} cells compared with controls. ALDH1^{+} and ALDH1^{-} populations of SUM149 EZH2 KD or control cells were isolated by flow cytometry, and 1×10^4 cells were injected into the cleared mammary fat pads of NOD/SCID mice (10 per group). Kaplan–Meier plot shows that EZH2 KD significantly increases the time to tumor initiation in SUM149 ALDH1^{+} cells compared with controls (log-rank $P = 0.0019$). (*D*) Immunoblots of MDA-MB-231 and SUM149 cells show that EZH2 KD reduces the expression of the intracellular activated form of NOTCH1, NICD1, and its downstream targets HES1 and Cyclin D1 compared with controls. (*E*) Immunoblots show that re-expression of EZH2 in EZH2 KD MDA-MB-231 and SUM149 cells rescues NICD1 levels. (*F*) Effect of EZH2 KD on the TIC population of cancer cells derived from a patient tumor (Tumor 1). Shown is a representative image of Tumor 1 stained with H&E and with an anti-EZH2 antibody. (Magnification: 400×.) Immunoblots show that EZH2 KD decreases NICD1 and HES1 expression compared with controls. EZH2 KD significantly decreases mammospheres and the percentages of ALDH1^{+} and CD44^{+}/CD24^{-} cells compared with controls ± SD (*t* test: $*P < 0.0001$, $*P = 0.01$, and $*P = 0.002$, respectively). (*G*) Effect of EZH2 KD on the TIC population of cancer cells derived from another patient tumor (Tumor 2). EZH2 KD decreases NICD1 and HES1 expression and reduces the CD44^{+}/CD24^{-} population compared with controls ± SD (*t* test, $*P = 0.008$). (*H*) Expression of constitutively active NICD1 in cells derived from Tumor 1 rescues the effect of EZH2 KD on TICs (*t* test: $*P = 0.0004$; $**P = 0.002$).

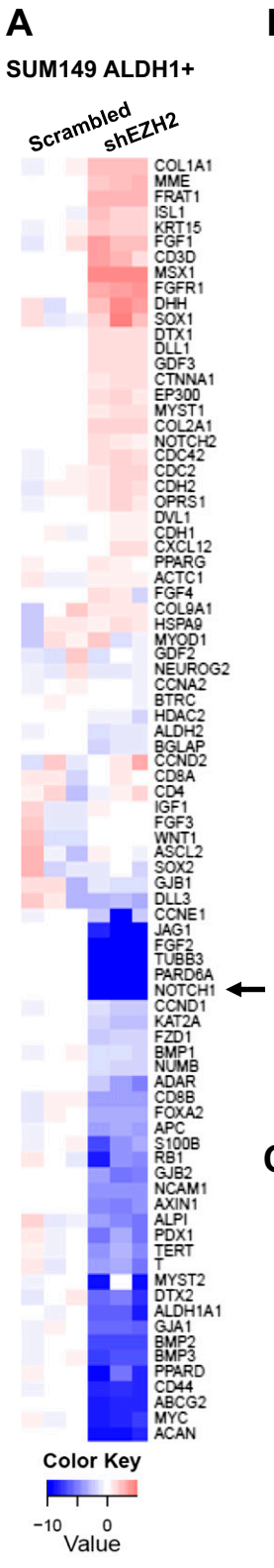

B

Fold Difference of SUM149 Scrambled/shEZH2

Gene	ALDH1-	ALDH1+
ABCG2	70.64	319.00
ACTC1	46.11	0.70
ADAR	8.56	12.40
ACAN	0.91	469.00
ALDH1A1	1.40	79.10
ALDH2	0.42	2.09
ALPI	1.40	21.10
APC	1.72	12.04
ASCL2	0.18	1.18
AXIN1	3.22	24.20
BGLAP	0.37	2.40
BMP1	0.76	3.10
BMP2	0.08	119.60
BMP3	4.96	70.20
BTRC	0.63	1.32
CCNA2	1.15	0.01
CCND1	2.18	3.88
CCND2	0.32	0.35
CCNE1	4.10	78.10
CD3D	0.73	0.14
CD4	1.35	0.83
CD44	0.65	256.00
CD8A	2.10	0.69
CD8B	0.64	15.10
CDC2	0.42	0.35
CDC42	1.20	0.34
CDH1	0.64	0.77
CDH2	1.18	0.40
COL1A1	0.04	0.15
COL2A1	197.64	0.30
COL9A1	1.44	0.74
CTNNA1	0.58	0.40
CXCL12	0.64	0.40
DHH	1.53	0.09
DLL1	4.62	0.40
DLL3	1.13	3.31
DTX1	0.64	0.40
DTX2	1.93	71.32
DVL1	0.62	0.67
EP300	2.81	0.39
FGF1	0.64	0.30
FGF2	164.41	1718.80

Gene	ALDH1-	ALDH1+
FGF3	0.64	0.95
FGF4	0.48	0.44
FGFR1	0.64	0.07
FOXA2	0.00	9.39
FRAT1	22.01	0.12
FZD1	0.84	4.05
KAT2A	4.17	4.79
GDF2	2.52	1.10
GDF3	0.64	0.41
GJA1	12.40	65.00
GJB1	4.57	2.70
GJB2	1.03	25.30
HDAC2	1.84	1.90
HSPA9	0.74	0.50
IGF1	2.49	0.79
PDX1	7.18	11.50
ISL1	0.16	0.24
JAG1	1540.74	977.00
KRT15	0.77	0.26
MME	0.12	0.16
MSX1	0.20	0.04
MYC	53.13	238.00
MYOD1	0.77	0.72
MYST1	0.30	0.40
MYST2	21.57	66.00
NCAM1	40.75	17.20
NEUROG2	0.93	0.81
NOTCH1	18.19	9687.00
NOTCH2	0.59	0.50
NUMB	2.12	3.13
SIGMAR1	0.49	0.45
PARD6A	0.83	5603.00
PPARD	0.36	203.00
PPARG	0.16	0.67
RB1	2.94	54.60
S100B	1.59	28.50
SOX1	0.82	0.11
SOX2	0.71	1.00
T	0.29	12.30
TERT	1.80	15.20
TUBB3	0.72	4781.00
WNT1	1.82	1.14

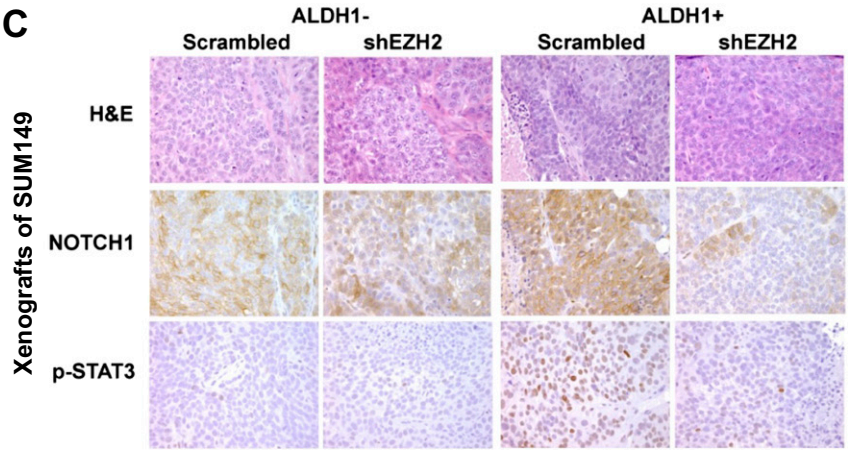

Fig. S2. EZH2 KD in ALDH1$^+$ and ALDH1$^-$ populations of SUM149 cells deregulates genes involved in stem cell biology. (*A*) Heat map of quantitative (q) RT-PCR microarray (SABiosciences Stem Cell PCR Array) using mRNA isolated from SUM149 ALDH1$^+$ cells expressing EZH2-targeted (shEZH2) or scrambled control shRNA. (*B*) Complete list of genes analyzed using mRNA and the microarray as described in *A*. Shown are fold-differences in mRNA expression comparing the ALDH1$^-$ and ALDH1$^+$ populations. *NOTCH1* was one of the most significantly down-regulated genes by EZH2 KD in the ALDH1$^+$ population compared with the ALDH1$^-$ cells (9,687 fold vs. 18 fold, respectively; *t* test, $P < 0.00001$). (*C*) Representative images of xenografts derived from the ALDH1$^+$ and ALDH1$^-$ populations of SUM149 EZH2 KD or control cells. EZH2 KD decreased the expression of total NOTCH1 and its target, phosphorylated STAT3 (p-STAT3), in xenografts derived from ALDH1$^+$ cells but not in tumors derived from ALDH1$^-$ cells. (Magnification 400×.)

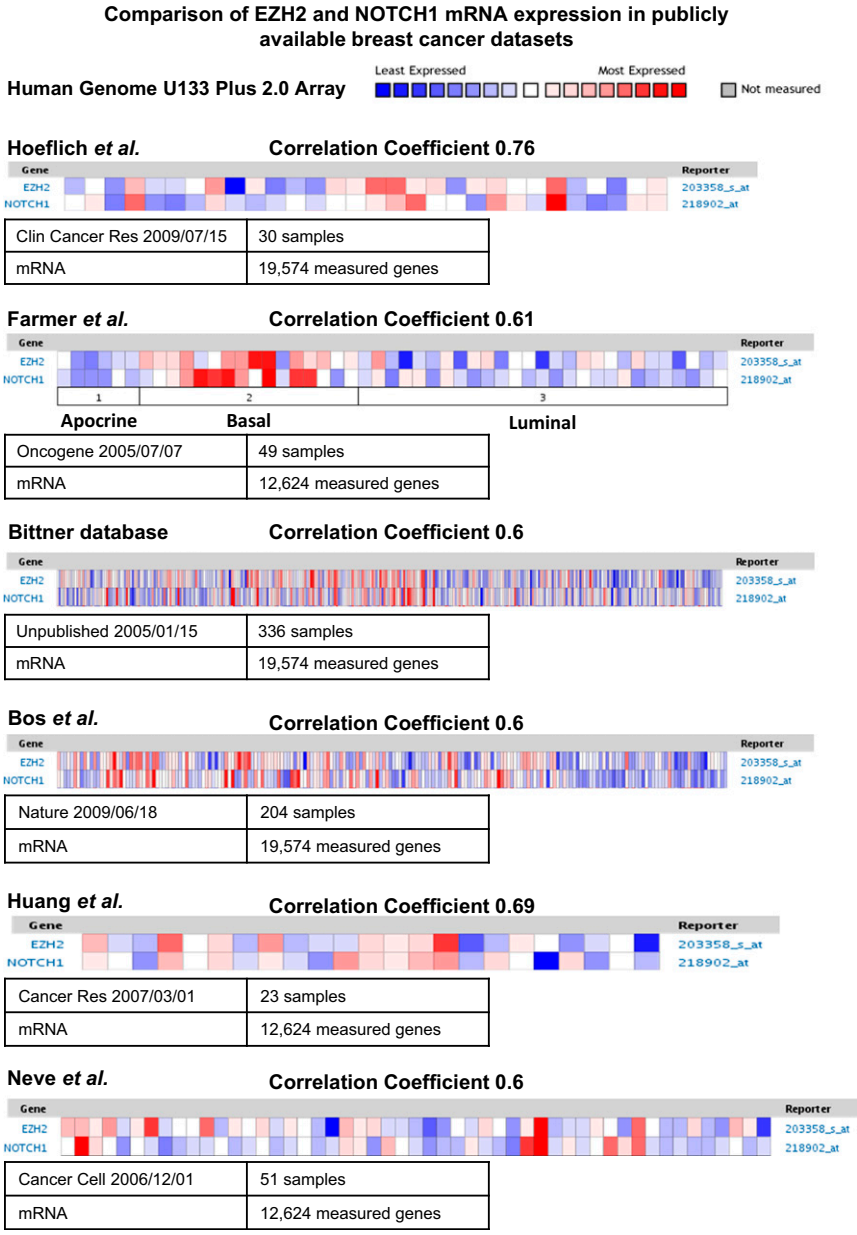

Fig. S3. *EZH2* mRNA expression is associated with *NOTCH1* mRNA levels in independent datasets of invasive breast carcinomas from patients. We identified a significant association between *EZH2* and *NOTCH1* mRNA expression levels in publicly available datasets of human breast cancer and breast cancer cell lines using Oncomine.

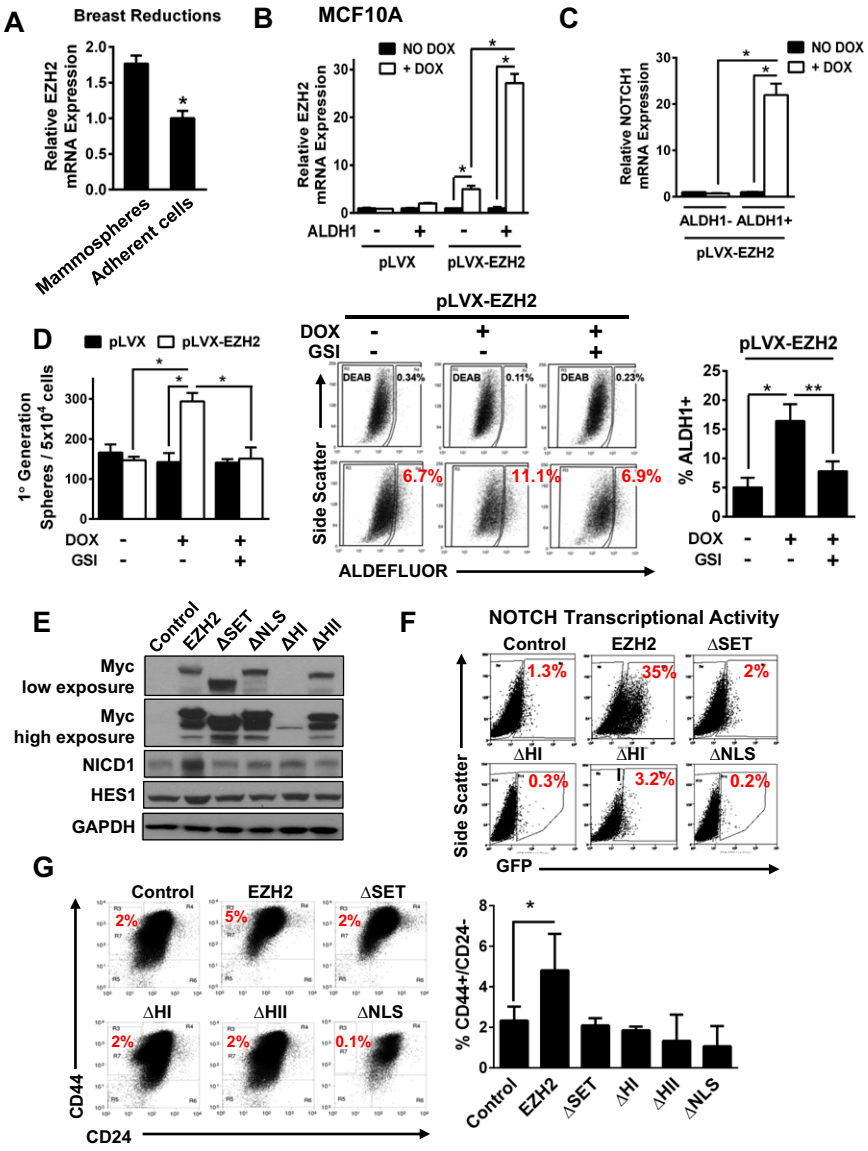

Fig. S4. NOTCH pathway activation is required for EZH2-mediated stem cell expansion. (*A*) Quantitative RT-PCR reveals that *EZH2* mRNA expression of nontumorigenic primary breast cells obtained from reduction mammoplasties is elevated in the mammosphere forming population compared with adherent cell cultures (*t* test, $*P < 0.0001$). (*B*) MCF10A pLVX (control) and pLVX-EZH2 (inducible) cells untreated or treated with doxycycline (DOX) (500 ng/mL for 24 h) were sorted using the ALDEFLUOR assay and subjected to qRT-PCR. DOX significantly increases *EZH2* mRNA levels in ALDH1$^+$ and ALDH1$^-$ pLVX-EZH2 cells, and the EZH2 mRNA is significantly higher in ALDH1$^+$ compared with ALDH1$^-$ cells (*t* test, $*P < 0.0001$). (*C*) DOX-induced EZH2 overexpression in MCF10A$^-$ pLVX-EZH2 cells increases *NOTCH1* mRNA levels in ALDH1$^+$ cells compared with ALDH1$^-$ cells (*t* test, $*P = 0.0001$). (*D*, *Left*) DOX-induced overexpression of EZH2 in MCF10A pLVX-EZH2 cells significantly increases mammosphere numbers in the primary generation compared with controls, which is blocked with GSI treatment (1.7 nM for 7 d), added 24 h before DOX. Average sphere numbers per 5×10^4 plated cells ± SD (*t* test, $*P < 0.0001$). (*D*, *Right*) DOX-induced EZH2 overexpression in MCF10A pLVX-EZH2 cells leads to a significant increase in the percentage ALDH1$^+$ cells compared with controls, which is prevented by GSI treatment. Percentages are expressed ± SD (*t* test: $*P = 0.008$; $**P = 0.02$). (*E*) Immunoblots of MCF10A cells infected with adenovirus containing full-length EZH2, EZH2 deletion mutants, or adenovirus control probed with anti-NICD1 and anti-HES antibodies. (*F*) GFP-NOTCH promoter reporter assay of MCF10A cells overexpressing full-length EZH2, EZH2 deletion mutants, or controls. Full-length EZH2 is required to induce NOTCH transcriptional activity. Transcriptional activity was measured as the percentage of GFP-expressing cells ± SD by flow cytometry. (*G*) Flow cytometry using CD24 and CD44 antibodies show that full-length EZH2, but none of the deletion mutants, is required for the EZH2-induced expansion of the CD44$^+$/CD24$^-$ population. Bar graph shows the percentages ± SEM (*t* test, $*P < 0.005$).

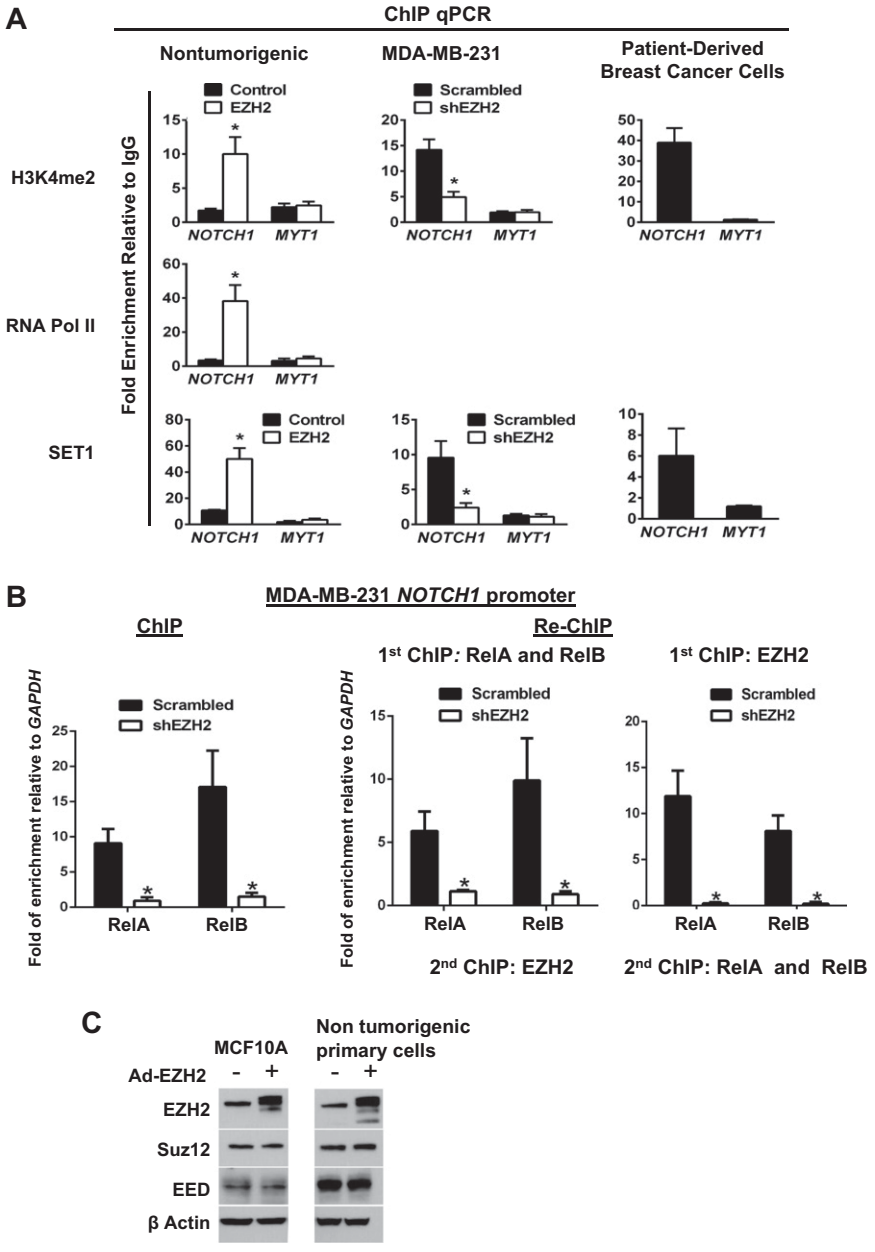

Fig. S5. EZH2 binding to the *NOTCH1* promoter is associated with H3K4me2, SET1 H3K4 methyltransferase, RNA Pol II binding, and interaction with RelA/RelB. (*A*) ChIP assays performed using qRT-PCR on nontumorigenic primary breast cells overexpressing full-length EZH2 or controls, on MDA-MB-231 breast cancer cells with EZH2-targeted or scrambled shRNAs, and on primary breast cancer cells, using anti-H3K4me2, anti-SET1, and anti-RNA Pol II. MYT1, positive binding control. (*B*, *Left*) ChIP assays on MDA-MB-231 cells with EZH2-targeted or scrambled shRNAs using anti-RelA and anti-RelB. (*B*, *Right*) Re-ChIP assays of EZH2, RelA, and RelB. First ChIP and second ChIP antibodies are indicated at the chart title and *x*-axis labels, respectively. Bar graphs represent three independent experiments ± SEM (*t* test, $*P < 0.05$). (*C*) Western blot analyses of indicated proteins in MCF10A and nontumorigenic primary breast cells overexpressing EZH2 or control.

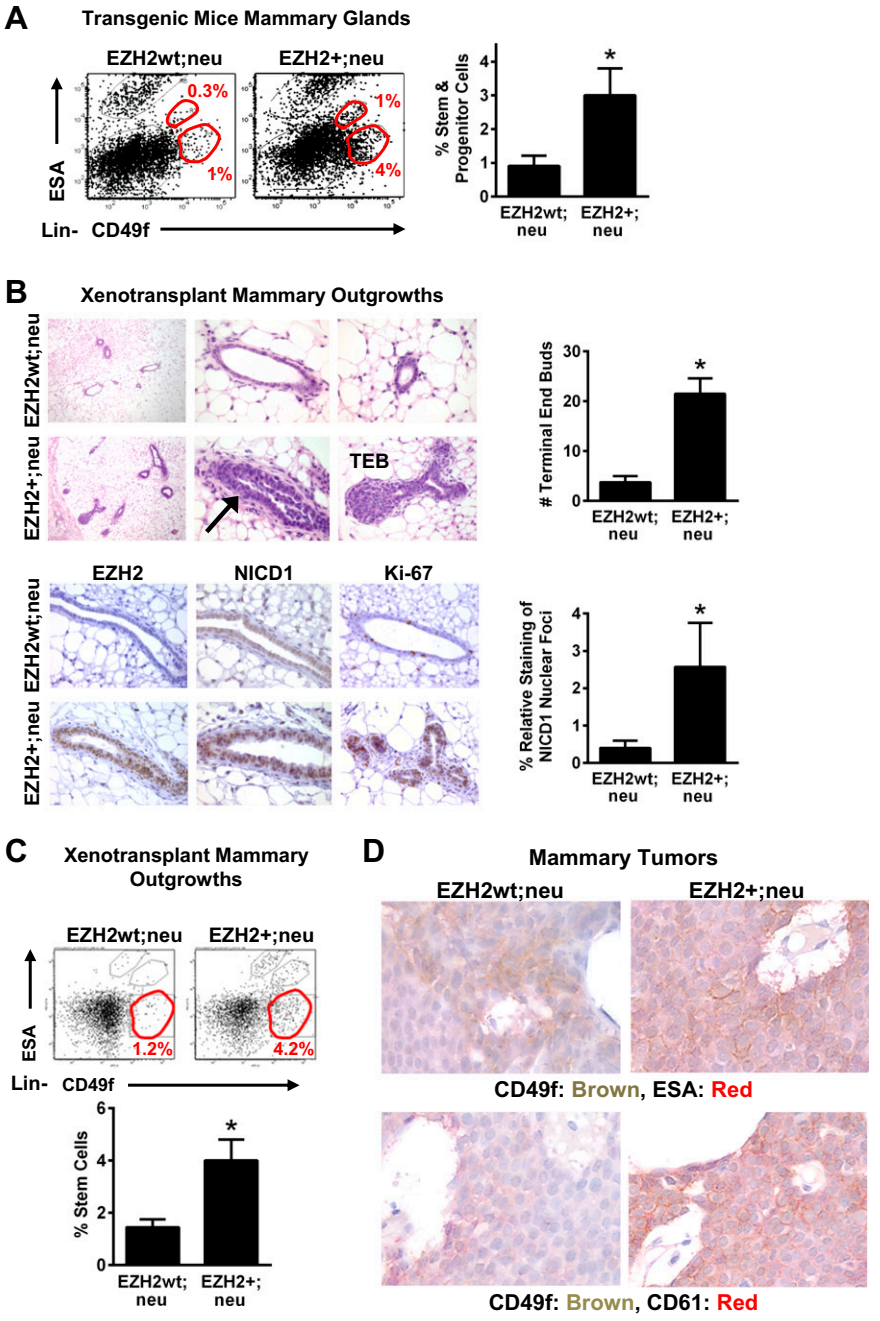

Fig. S6. Transgenic EZH2 overexpression expands the stem cell population in preneoplastic mammary glands and tumors of MMTV-neu mice. (*A*) Flow cytometric analysis of 8-wk-old virgin mice in the Lin^- population using ESA and CD49f antibodies, shown to identify stem and progenitor populations in human and in MMTV-neu mammary glands (16, 17), reveal that transgenic overexpression of EZH2 induced an increase in the percentage of stem (Lin^- ESA^{med} $CD49f^{high}$) and progenitor cells (Lin^- ESA^{high} $CD49f^{med}$) compared with controls ± SEM (Student *t* test, $*P = 0.05$). (*B*) Mammary stem and progenitor cells of 8-wk-old $EZH2^+$;neu and $EZH2^{wt}$;neu virgin mice (5,000 cells per group) were independently transplanted into the cleared fat pads of syngeneic 3-wk-old FBV mice ($n = 15$ per group) (15). After a 5 wk observation period, mammary glands were excised and used for subsequent experiments. Stem cells of $EZH2^+$;neu and $EZH2^{wt}$;neu mice exhibited mammary repopulating capacity evidenced by the formation of mammary outgrowths. Shown are representative histopathological images of H&E-stained outgrowths following transplantation of stem cells from $EZH2^{wt}$;neu and $EZH2^+$;neu mammary glands. (Magnification: 400×.) Outgrowths from the $EZH2^+$;neu group exhibited pronounced intraductal hyperplasia (black arrow) similar to human disease. We also noted increased numbers of terminal end buds (TEBs) compared with $EZH2^{wt}$;neu outgrowths ± SD (Student *t* test, $*P < 0.0001$). Mammary outgrowths were stained for EZH2, NICD1, and the proliferation marker Ki-67. Ductal epithelial cells from $EZH2^+$;neu outgrowths exhibit EZH2 overexpression, significantly increased NICD1 nuclear protein expression ± SD (Student *t* test, $*P < 0.03$), and marked increase in proliferation compared with controls. (Magnification: 400×.) (*C*) FACS analyses performed in triplicate show that $EZH2^+$;neu outgrowths contain a higher percentage of stem cells (Lin^- ESA^{med} $CD49f^{high}$) compared with $EZH2^{wt}$;neu outgrowths ± SEM (Student *t* test, $*P = 0.05$). (*D*) $EZH2^+$;neu tumors exhibit larger areas containing cells coexpressing CD49f/ESA and CD49f/CD61 compared with $EZH2^{wt}$;neu tumors. Dual-immunohistochemistry assays to detect CD49f/ESA and CD49f/CD61 in the mammary tumors were developed in our laboratory; CD49f is brown and ESA or CD61 are red. These markers have been shown by flow cytometry to detect the TIC population in MMTV-neu neoplastic progression (17). Representative images of $EZH2^+$;neu and $EZH2^{wt}$;neu tumors are shown ($n = 5$ per condition). (Magnification: 600×.)

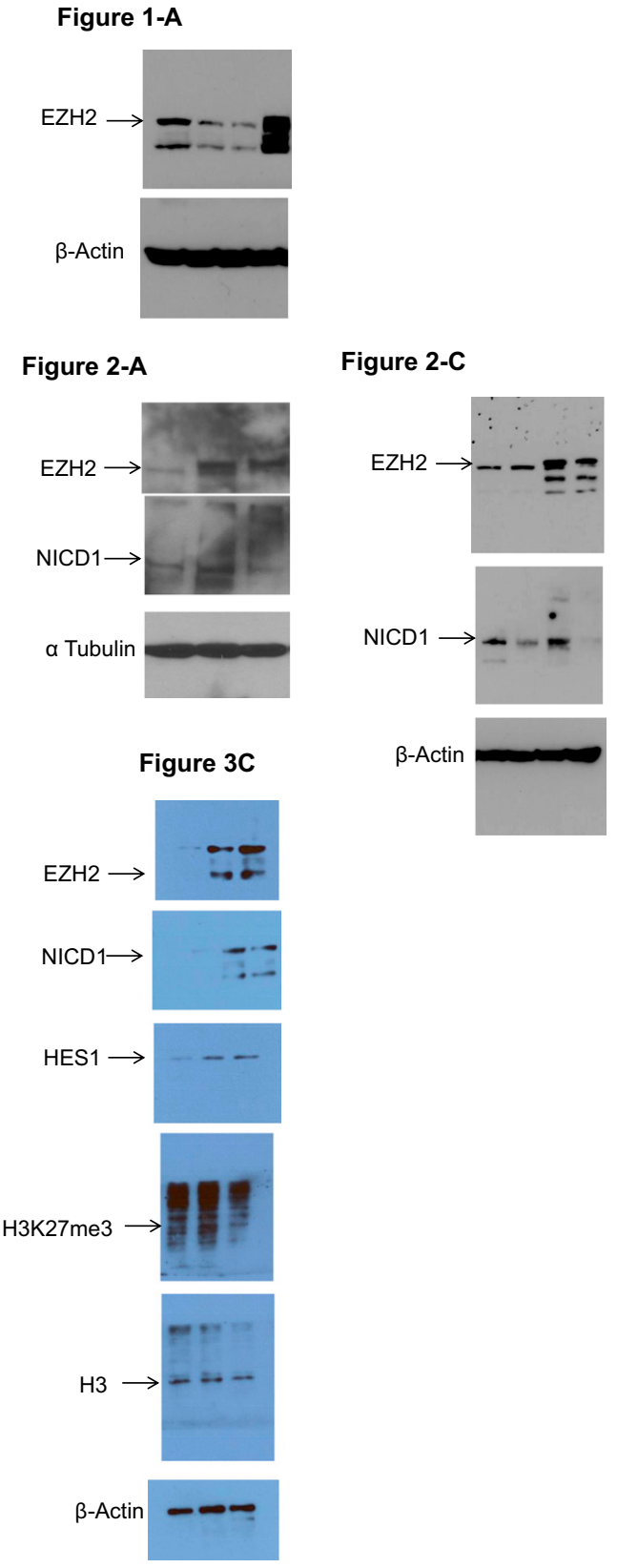

Fig. S7. (Continued)

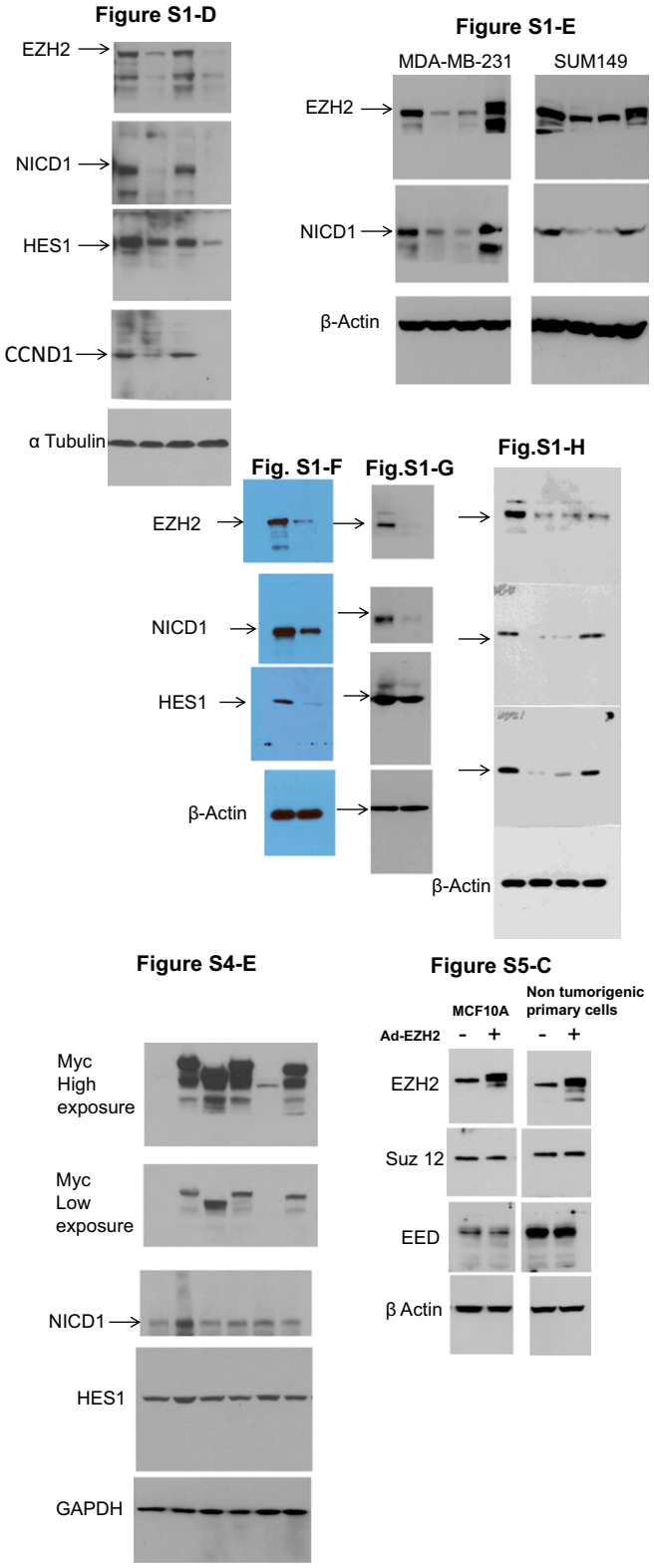

Fig. S7. Expanded regions from immunoblot films for all Western blot experiments presented.

Table S1. Number of mice with mammary tumors after injection of ALDH1$^+$ and ALDH1$^-$ populations of SUM149 cells expressing EZH2-targeted or scrambled shRNA

	No. of mice with tumors/total mice					
SUM149 Cells	Week 5	Week 6	Week 7	Week 8	Week 9	Week 10
ALDH1$^-$						
Scrambled	0/9 (0%)	2/9 (22%)	5/9 (56%)	7/9 (78%)	9/9 (100%)	9/9 (100%)
shEZH2	0/8 (0%)	0/8 (0%)	2/8 (25%)	5/8 (63%)	6/8 (75%)	6/8 (75%)
ALDH1$^+$						
Scrambled	2/9 (22%)	5/9 (56%)	9/9 (100%)	9/9 (100%)	9/9 (100%)	9/9 (100%)
shEZH2	0/10 (0%)	2/10 (20%)	5/10 (50%)	7/10 (70%)	7/10 (70%)	8/10 (80%)

χ^2 test: $P < 0.0001$.

Table S2. Associations between EZH2 and NICD1 (EZH2^{high}/NICD1$^+$) and breast cancer features

Characteristic	No ($n = 75$)	Yes ($n = 68$)	P*
CD44$^+$/CD24$^-$			
No	38 (50.7%)	22 (32.3%)	0.0008
Yes	14 (18.7%)	32 (47.1%)	
Unknown	23 (30.7%)	14 (20.6%)	
Tumor histological grade			
I or II	35 (46.7%)	17 (25.0%)	0.0064
III	33 (44.0%)	44 (64.7%)	
Unknown	7 (9.3%)	7 (10.3%)	
Molecular type			
Luminal	42 (56.0%)	25 (36.8%)	0.0029
Triple negative	23 (30.7%)	35 (51.5%)	
HER2	4 (5.3%)	5 (7.4%)	
Unknown	6 (8.0%)	3 (4.4%)	

*χ^2 test of independence.